


RESEARCH ARTICLE OPEN ACCESS

Overproduction and Characterization of Recombinant Soluble *Trypanosoma brucei* Phospholipase A₂

Oluwafemi Abiodun Adepoju^{1,2}  | Daniel Quinnell² | Harshverdhan Sirohi² | Emmanuel Amlabu^{3,4} | Abdullahi Balarabe Sallau^{1,4} | Abdulrazak Ibrahim^{1,5} | Sunday Ene-Ojo Atawodi⁶ | Mohammed Nasiru Shuaibu^{1,4} | Geoffrey Chang^{2,7} | Emmanuel Oluwadare Balogun^{1,2,4,8}

¹Department of Biochemistry, Ahmadu Bello University, Zaria, Nigeria | ²Skaggs School of Pharmacy and Pharmaceutical Sciences, University of California San Diego, La Jolla, California, USA | ³Department of Biochemistry, Prince Abubakar Audu University, Anyigba, Nigeria | ⁴Africa Centre of Excellence for Neglected Tropical Diseases and Forensic Biotechnology, Ahmadu Bello University, Zaria, Nigeria | ⁵Forum for Agricultural Research in Africa (FARA), PMB CT 173, Cantonments, Accra, Ghana | ⁶Department of Biochemistry, Federal University Lokoja, Lokoja, Kogi, Nigeria | ⁷Department of Pharmacology, School of Medicine, University of California San Diego, La Jolla, California, USA | ⁸Department of Biomedical Chemistry, Graduate School of Medicine, The University of Tokyo, Hongo, Tokyo, Japan

Correspondence: Emmanuel Oluwadare Balogun (oluwadareus@yahoo.com)

Received: 7 October 2024 | **Revised:** 17 December 2024 | **Accepted:** 17 January 2025

Funding: This study was funded by Fogarty International Center of the National Institutes of Health under award number K43TW012015.

Keywords: kinetoplastids | neglected tropical diseases | recombinant DNA technology | *Trypanosoma brucei* phospholipase A₂ | trypanosomiasis

ABSTRACT

Trypanosoma brucei phospholipase A₂ (TbPLA₂) is a validated drug target but the difficulty in expressing its soluble recombinant protein has limited its exploitation for drug and vaccine development for African and American trypanosomiasis. We utilized recombinant deoxyribonucleic acid (DNA) technology approaches to express soluble TbPLA₂ in *Escherichia coli* and *Pichia pastoris* and biochemically characterize the purified enzyme. Full-length TbPLA₂ was insoluble and deposited as inclusion bodies when expressed in *E. coli*. However, soluble and active forms were obtained when both the full-length and truncated TbPLA₂ were expressed in fusion with N-terminal FLAG tag and C-terminal eGFP in *P. pastoris*, and the truncated protein in fusion with N-terminal FLAG tag and C-terminal mClover in *E. coli*. Truncated TbPLA₂ lacking the signal peptide and transmembrane domain was finally expressed in Rosetta 2 cells and purified to homogeneity. Its migration on sodium dodecyl polyacrylamide gel electrophoresis (SDS-PAGE) confirmed its size to be 39 kDa. Kinetic studies revealed that the enzyme has a specific activity of 107.14 μmol/min/mg, a V_{\max} of 25.1 μmol/min, and a K_M of 1.58 mM. This is the first report on the successful expression of soluble and active recombinant TbPLA₂, which will facilitate the discovery of its specific inhibitors for the development of therapeutics for trypanosomiasis.

1 | Introduction

African trypanosomiasis (AT) is a parasitic disease caused by multiple species of trypanosomes and transmitted by insect

vectors, mostly the *Glossina* genus [1]. This disease affects humans and animals in sub-Saharan Africa, negatively impacting the economic stability and well-being of the people. Animal African trypanosomiasis (AAT) causes a loss of ~\$5 billion (USD)

Abbreviations: DNA, deoxyribonucleic acid; IPTG, isopropyl-β-D-thiogalactopyranoside; PLA₂, phospholipase A₂; SDS-PAGE, sodium dodecyl polyacrylamide gel electrophoresis; TbPLA₂, *Trypanosoma brucei* phospholipase A₂; TEV, tobacco etch virus.

This is an open access article under the terms of the [Creative Commons Attribution-NonCommercial](https://creativecommons.org/licenses/by-nc/4.0/) License, which permits use, distribution and reproduction in any medium, provided the original work is properly cited and is not used for commercial purposes.

© 2025 The Author(s). *Engineering in Life Sciences* published by Wiley-VCH GmbH.

Summary

- This research provides a unique opportunity to develop therapeutics targeting *Trypanosoma brucei* phospholipase A₂ (TbPLA₂), a validated drug target.
- We successfully produced soluble and functional recombinant TbPLA₂ for the first time, paving the way for discovering specific inhibitors crucial for innovative, low-toxicity treatments for sleeping sickness, Chagas disease, and Leishmaniasis.
- The production of functional recombinant TbPLA₂ offers promising prospects for drug and vaccine development against these diseases, identified by the WHO as critical neglected tropical diseases (NTDs) targeted for elimination by 2030.
- Future studies can now focus on developing novel solutions, whether drugs or vaccines, that target *Trypanosoma* PLA₂ for the control and elimination of trypanosomiasis.

annually, contributing to economic strain and underdevelopment of the African continent [2]. Human African trypanosomiasis (HAT) threatens about 70 million people living in sub-Saharan Africa and kills about 4000 people annually [3, 4]. There are currently no vaccines to prevent infection, and the available drugs are unsatisfactory due to toxicity and treatment failure. Trypanosomiasis and other vector-borne diseases continue to spread to nonendemic countries through livestock trade and vector migration due to climate change [5, 6], hence, the need for intervention approaches.

Trypanosomes undergo adaptations during their lifecycle to acquire features that will fit them for survival in their next host environment. They undergo membrane phospholipids remodeling which is solely mediated by phospholipases [7–9]. Furthermore, they do not synthesize arachidonic acid (AA) de novo but rely on exogenous supply from their hosts by cleaving the fatty acyl on the *sn*-2 carbon of the host's phospholipid glycerol backbone with their phospholipase A₂ (PLA₂) to release AA (Figure S1). The AA is a second messenger that regulates Ca²⁺ homeostasis and a precursor of prostaglandins (PGDs) which are virulent factors that interfere with the host immune system to promote infection. PGDs are involved in the regulation of differentiation and development of trypanosomes [10–12]. The central roles of PLA₂ in the infectivity, cell invasion, virulence, pathogenesis, and maintenance of pathogenic protozoans in their hosts have been well demonstrated by investigators [13–15], validating it as an attractive therapeutic target.

PLA₂ is conserved across all domains of life; however, whereas the identity amongst some medically important kinetoplastids species is high (85%–99%), *Trypanosoma brucei* PLA₂ (TbPLA₂) is substantially different from mammalian PLA₂ (~34%) (Table S1). The critical role of PLA₂ in the lipid metabolism of trypanosomes makes it essential for their survival [11, 16]. The inhibition of PLA₂ has been demonstrated to cause the death of *T. b. brucei*, *T. b. gambiense*, and *Leishmania amazonensis*, validating it as a potential drug target across the kinetoplastids [15, 17, 18]. The similarity of kinetoplastids PLA₂s and their differences from

the mammalian homologs can be exploited for the development of broad-acting therapeutics against kinetoplastids. Although a PLA₂-like gene sequence exists in the genome of trypanosomes, overexpression of the functional enzyme has been flawed by its insolubility, hence the lack of enzymological data. This problem has limited the exploitation of TbPLA₂ for drug or vaccine development to date. As a step to solve this problem, we employed recombinant deoxyribonucleic acid (DNA) technology and biophysical approaches to successfully produce soluble and functional TbPLA₂ protein in milligram quantity. Our findings will form a basis for the development of therapeutics that spare mammalian PLA₂ but specifically target TbPLA₂ for the treatment of AT.

2 | Materials and Methods

2.1 | Competent Cells and Vectors

Plasmids were propagated in OneShot TOP10 chemically competent *Escherichia coli* cells (ThermoFisher, USA). Chemically competent BL21-CodonPlus (DE3)-RIL, BL21-CodonPlus (DE3)-RIPL, ArcticExpress (DE3), BL21 (DE3) pLysS (Agilent, USA), Rosetta 2 (DE3) (Novagen, USA), and electrocompetent *Pichia pastoris* KM71H strain (ThermoFisher, USA) were used for protein expression (Table S2).

2.2 | Bioinformatics Analysis, Codon Optimization, Synthesis, and Subcloning of *tbpla2*

Sequences of human and trypanosomes PLA₂s were retrieved from the NCBI website and used for multiple sequence alignment (Figures S2 and S3). The TbPLA₂ sequence was submitted to the TMHMM and I-TASSER servers for the prediction of trans-membrane (TM) helices and the 3D structure of the protein, respectively [19–22]. The *tbpla2* was codon-optimized, synthesized, and subcloned into pET-24b(+) using *XhoI* and *NdeI* restriction sites (GenScript, USA). Subcloning was confirmed by digesting 300 ng of the pET-24b(+)-TbPLA₂ by *XhoI* and *NdeI* at 37°C for 4 min. The product was analyzed on 1% agarose gel. The orientation of the insert was confirmed by Sanger sequencing (GenScript, USA).

2.3 | Subcloning of *tbpla2* Constructs Into pFLAG and pPICZ

Constructs of *tbpla2* were subcloned into pFLAG and pPICZ vectors. The pFLAG vector is a custom-designed construct, created in our laboratory from the pMBP plasmid backbone. It contains a tac promoter and a *lacI^q* promoter, a stronger repressor (10× more than *lacI*) of the lac promoter. The pPICZ contains an AOX1 promoter that is inducible by methanol. Primers were designed on SnapGene (Table S3) and synthesized by IDT and ThermoFisher (USA). Overhang sequences were included in the *tbpla2* primers for Gibson or HiFi assembly. Linearization of the plasmids and amplification of *tbpla2* were done by PCR. Truncated *tbpla2* lacking the signal peptide and TM sequences were generated by PCR using primers designed to exclude the signal peptide and TM sequences. The linearized plasmids and

tbpla2 amplicons were resolved on 1% agarose gel, excised, and purified using the GeneJET Gel Extraction Kit (ThermoFisher, USA). The plasmid was ligated with the *tbpla2* construct by Gibson or HiFi assembly (New England Biolabs, USA) [23] and transferred on ice for the transformation of chemically competent *E. coli* cells by heat shock or electrocompetent *P. pastoris* by electroporation. Both plasmids have an FLAG tag at the N-terminus and either a mClover or eGFP at the C-terminus in the pFLAG and pPICZ, respectively. FLAG tag allows affinity purification of the recombinant protein on anti-FLAG M2 resin, and detection by western blot using anti-FLAG antibody. The eGFP and mClover tags are fluorescent and can be used to monitor expression. The constructs were sequenced to verify subcloning and the correct orientation of the inserts (Genewiz, USA).

2.4 | Expression of TbPLA₂ in *E. coli*

Optimization of protein expression was carried out at varying temperatures and isopropyl- β -D-thiogalactopyranoside (IPTG) concentrations (Table S4). Each of the competent *E. coli* cells was transformed by heat shock [24], and grown on LB agar plates containing the appropriate antibiotic (kanamycin, 50 μ g/mL; carbenicillin, 100 μ g/mL; ampicillin, 100 μ g/mL). A single colony from the plate was used to inoculate 10 mL of LB or terrific broth (TB) containing the appropriate antibiotic. The culture was grown overnight at 37°C with shaking at 225 rpm. The overnight culture was used to inoculate 1 L media flasks which were grown and induced with IPTG at OD₆₀₀ of 0.8 and a temperature of 20°C. The cells were harvested 18 h postinduction and stored at -80°C. For large-scale expression, 300 mL from the 1 L flasks were used to inoculate 10 L TB medium containing antifoam and the appropriate antibiotic in New Brunswick Scientific BioFlo 415 fermenters. The dissolved oxygen (DO) span was set to 100%, and the RPM was set to 300. The DO was cascaded to RPM at 30% with a maximum RPM set to 700. When the DO reached 30% at an OD₆₀₀ of approximately 1.2, the fermenters were induced with 0.1 mM IPTG. The cells were harvested 18 h postinduction and stored at -80°C.

2.5 | Expression of TbPLA₂ in *Pichia pastoris*

Chemically competent TOP10 *E. coli* cells were transformed with the recombinant pPICZ plasmid containing the *tbpla2* insert and grown on low-salt LB plates supplemented with 25 μ g/mL zeocin. A single colony from the plate was used to inoculate 10 mL of LB medium containing 25 μ g/mL zeocin, from which the plasmid was subsequently extracted and purified. Exactly 2 μ g of the plasmid was linearized by *PmeI* (New England Biolabs, USA) and transformed into electrocompetent *P. pastoris* KM71H cells by electroporation [25]. The electroporated cells were allowed to recover in 1 M sorbitol at 30°C for 1 h. An equal volume of 2× YPD was added, and the cells were incubated for 3 h at 30°C. The cells were then plated on YPD agar plates containing 1 M sorbitol and zeocin (200, 500, and 1000 μ g/mL), and incubated for 3 days at 30°C. Single colonies from the plates were selected for mini-expression in 96-well blocks by methanol induction. Clones expressing TbPLA₂-eGFP were selected by fluorescence and used for large-scale production of recombinant TbPLA₂

using a protocol earlier described [25]. The fermenters were preequilibrated with O₂, and the cells were grown at pH 5.0 and a temperature of 28°C (gas flow: 4 LPM, O₂ span: 100%, DO: 10). Protein expression was carried out by slow methanol induction for 18 h (gas flow: 25 LPM, DO: 50). The cells were harvested and stored at -80°C.

2.6 | Purification of TbPLA₂

Frozen cell pellets were resuspended in lysis buffer (50 mM Tris, 300 mM NaCl, 5 mM CaCl₂, DNase; pH 8.0). For the *E. coli* pellets, 1× protease inhibitor cocktail (PIC) was added to the buffer while 25 mM benzamidine was used in the lysis buffer for the *P. pastoris*. Buffers for purification on Ni-NTA contained TCEP and imidazole. Lysis of *E. coli* cells was achieved by adding lysozyme and 1% Triton X-100 to the resuspended cells and stirring on a magnetic stirrer for 1 h at 4°C. The supernatant was recovered by centrifugation. Purification was done on an FPLC system or by gravity flow. Elution on the Ni-NTA column was done with 300 mM imidazole while 6 mg/mL FLAG peptide (pH 8.0) was used for elution on the anti-FLAG M2 column. The fractions were analyzed by sodium dodecyl polyacrylamide gel electrophoresis (SDS-PAGE) [26]. *P. pastoris* cells were lysed using a cell disruptor. To purify the full-length TbPLA₂, the membrane fraction (MF) was isolated by low-speed centrifugation. The full-length TbPLA₂ was then purified from the MF. For the truncated TbPLA₂, the supernatant was collected after high-speed centrifugation, from which the TbPLA₂ was purified. Fusion tags (eGFP and mClover) were removed by tobacco etch virus (TEV) cleavage at 4°C followed by a clean-up purification step on Ni-NTA column to isolate free TbPLA₂. Successful cleavage and purity were assessed by SDS-PAGE. Protein concentration was estimated on a nanophotometer at 280 nm using the extinction coefficient and molecular weight of TbPLA₂.

To prevent TbPLA₂ aggregation, seven detergents were screened by adding each to 0.50 mL of the purified TbPLA₂ in separate 30 kDa Amicon Ultra-0.5 Centrifugal Filters (Table S5). After concentration, the retentates were collected, and the filter membranes were washed with 1% SDS. The retentates and the washes were analyzed by SDS-PAGE.

2.7 | Solubility Test, Solubilization of Inclusion Bodies, and Refolding of TbPLA₂

Induced pLysS cell culture (1 mL) was centrifuged at 14,000 rpm for 5 min. The media was removed, and the cells were lysed by resuspension in RIPA buffer. The supernatant and pellet were analyzed by SDS-PAGE [27]. The recovered pellet (inclusion body) was solubilized with 4 M urea on a shaker at room temperature for 18 h, and the supernatant was purified on a Ni-NTA agarose column. Fractions were analyzed by SDS-PAGE. The optimum refolding condition of the TbPLA₂ purified from the inclusion bodies was determined using the Pierce Protein Refolding kit (ThermoFisher, USA). Restoration of disulfide linkages was confirmed by mobility shift SDS-PAGE/Western blot.

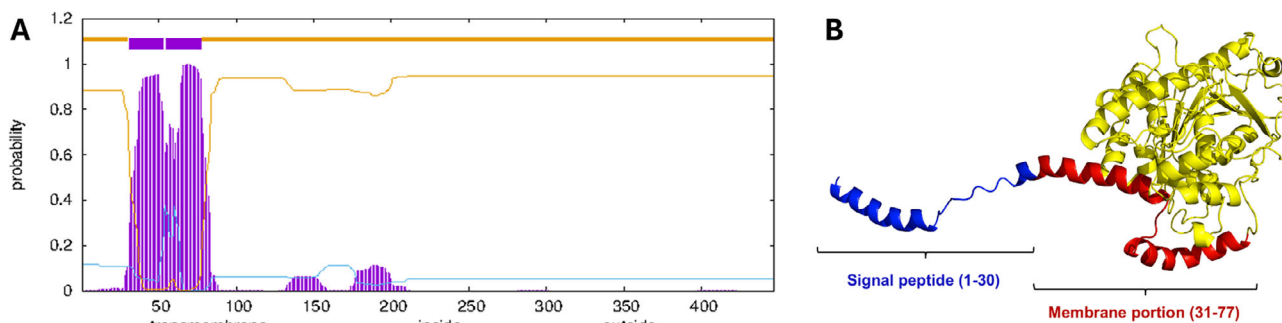


FIGURE 1 | Prediction of transmembrane helices and 3D structure of *Trypanosoma brucei* phospholipase A₂ (TbPLA₂): (A) Prediction of transmembrane helices of the full-length TbPLA₂ using the TMHMM server. TbPLA₂ is a 447-amino acid protein containing a signal peptide (1–30) and two transmembrane helices (TMHs) (31–77). The expected number of amino acids in the TMHs is 46.74769 and the expected number of TMHs amino acids in the first 60 amino acids is 23.62027. The total probability of having the N-terminal inside is 0.11760. (B) Predicted 3D structure of TbPLA₂ modeled on I-TASSER server showing the signal peptide (blue) and transmembrane domains (red).

2.8 | TbPLA₂ Activity Assay and Kinetics

The activity of TbPLA₂ was assessed as previously described with some modifications [28]. Briefly, 5 μ L (10 ng/ μ L) of TbPLA₂ was incubated with 45 μ L of 2 mg/mL L- α -lecithin at pH 8.0 and 37°C for 10 min. The reaction was stopped by heating to 99°C for 2 min. The AA released was titrated against 10 mM NaOH using phenolphthalein as an indicator. One unit of TbPLA₂ was defined as the amount of the enzyme that hydrolyzed 1.0 μ mole of L- α phosphatidylcholine to L- α -lysocleithin and AA per minute at pH 8.0 and temperature of 37°C. Determination of the kinetic parameters was carried out in triplicate, and reactions without the enzyme source were used as negative controls. Enzymatic activity was determined at varying concentrations of L- α phosphatidylcholine (0–8.0 mM) under predetermined optimum conditions (37°C, pH 8.0, and 50 ng TbPLA₂), and the data were used to determine the K_M and V_{max} by double reciprocal plot.

3 | Results

3.1 | Bioinformatics Analysis of TbPLA₂

Human PLA₂ differs significantly from trypanosomal PLA₂ (Table S1 and Figure S3). Notably, *T. b. gambiense* PLA₂ shares a high identity (>99%) with PLA₂s from *T. brucei* and *T. equiperdum* (*E* value: 0.0), and 60% identity with *T. congolense* PLA₂ (*E* value: 0.0). In contrast, TbPLA₂ and human PLA₂ exhibit 31.21% identity (*E* value: 3×10^{-12}). Figure 1 presents the predicted TM helices and 3D structure of TbPLA₂. The protein features a signal peptide (amino acids 1–30) and two TM helices (amino acids 31–77). The physiological variant spans amino acids 78–447. The signal peptide (blue) and the TM helices (red) can be identified in the predicted 3D structure.

3.2 | Synthesis and Subcloning of *tbpla2*

Figure 2A is the plasmid map of pET24b(+) containing the codon-optimized full-length *tbpla2*. The optimized TbPLA₂ has a codon adaptation index (CAI) of 0.9 and a GC content of 57%. The insert is flanked by *NdeI* and *XhoI* restriction enzyme sites. Digestion of pET24b(+)-TbPLA₂ by *NdeI* and *XhoI* showed that the *tbpla2*

insert migrated at 1344 bp (Figure 2B). The pET24b(+)-TbPLA₂ was used as the template in PCR reactions to amplify the TbPLA₂ constructs that were subcloned into pFLAG and pPICZ vectors. The electropherogram of the linearized pFLAG and pPICZ plasmids and *tbpla2* constructs is presented in Figure 2C. The linearized pFLAG (6299 bp) and the truncated *tbpla2* (1107 bp) were extracted from the gel and assembled using Gibson or HiFi assembly, likewise the linearized pPICZ vector (4062 bp) and the full-length (1338 bp) and truncated *tbpla2*. The final *tbpla2* construct that yielded TbPLA₂ with no signal peptide, TM domains, or fusion tag was generated from the pFLAG-TbPLA₂-mClover using primers that amplified the plasmid without the mClover sequence (Table S3). The resulting linear plasmid was ligated using KLD enzyme mix (NEB).

3.3 | Purification of TbPLA₂ Expressed in *E. coli* and *Pichia pastoris*

There was no visible expression of full-length TbPLA₂ in the RIL, RIPL, and Arctic Express cells (Figure 3A–C), but full-length TbPLA₂ was expressed as insoluble 39 and 58 kDa proteins in pLysS cells (Figure 3D). TbPLA₂ was not detected in the soluble fraction of the lysed RIPL cells (Figure 4A). Solubilization of the RIPL inclusion body using 4 M urea revealed the presence of degraded TbPLA₂, which was detected by Western blot using mouse anti-His monoclonal antibody (Figure 4B). Lysis of the induced pLysS cells using RIPA buffer did not release soluble TbPLA₂ as the protein remained in the pellet (Lane 2, Figure 4C), but its solubilization with 4 M urea released the 39 and 58 kDa proteins which were purified on Ni-NTA and analyzed by SDS-PAGE (Figure 4D). The optimum refolding condition of TbPLA₂ was established (55 mM Tris, 0.88 mM KCl, 21 mM NaCl, and pH 8.2) (Table S6 and Figure S4). Mobility shift SDS-PAGE of the reduced and non-reduced samples confirmed the renaturation of the disulfide linkages (Figure 4E).

Optimization of protein expression using the pLysS expression system showed that the *E. coli* expression system could not express soluble full-length TbPLA₂. The Rosetta 2 cells expressed soluble, truncated TbPLA₂ when IPTG induction was performed at 16 and 18°C. However, no protein expression was observed when induction was done at 37°C in the fermenter (Table S4).

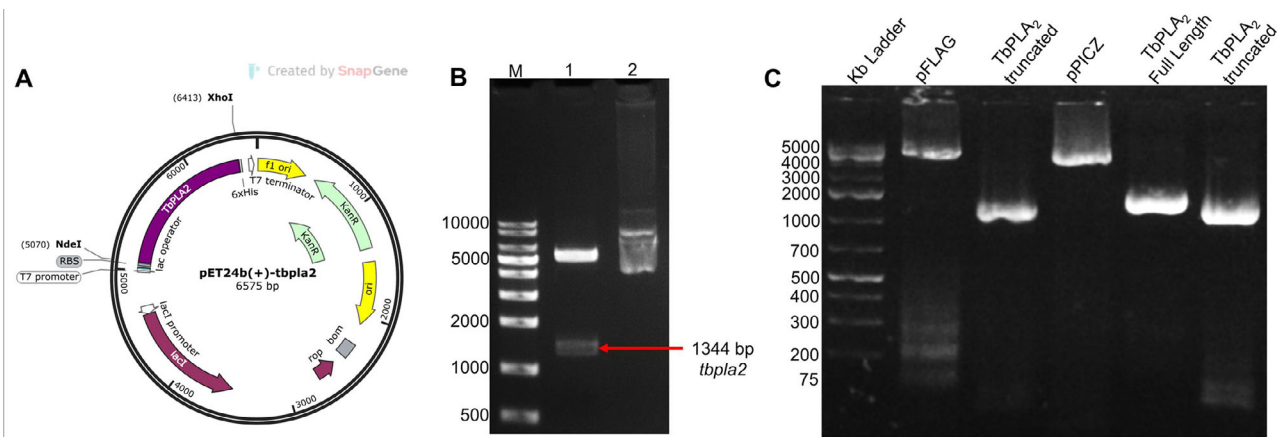


FIGURE 2 | Subcloning of *Trypanosoma brucei* phospholipase A₂ (*tbpla2*): (A) Plasmid map of pET-24b(+)-TbPLA₂. (B) Restriction enzyme digestion of pET-24b(+)-TbPLA₂ using XhoI and NdeI restriction enzymes. Lanes: M = KB ladder; 1 = pET-24b(+)-TbPLA₂ digested by NdeI and XhoI; 2 = undigested pET-24b(+)-TbPLA₂. Digestion was done with 300 ng of the plasmid incubated with NdeI and XhoI in a water bath at 37°C for 4 min. The products were analyzed on 1% agarose gel. (C) 1% w/v agarose gel electrophoresis of amplified plasmids and TbPLA₂ constructs.

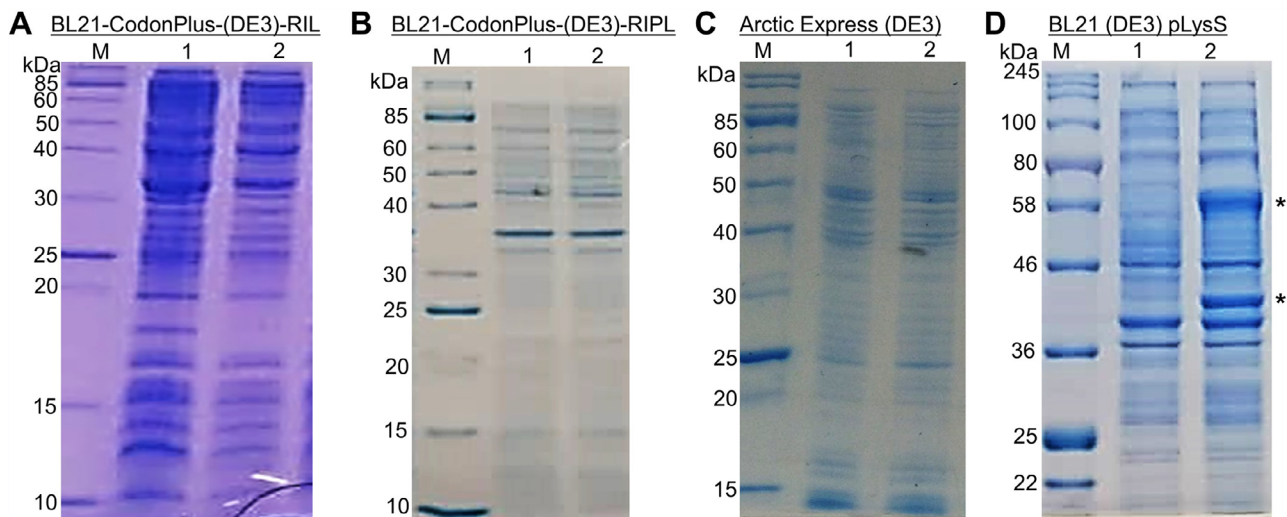


FIGURE 3 | Sodium dodecyl polyacrylamide gel electrophoresis (SDS-PAGE) of lysates from the expression of full-length *Trypanosoma brucei* phospholipase A₂ (TbPLA₂) in *E. coli* cells: (A) BL21-CodonPlus-(DE3)-RIL, (B) BL21-CodonPlus-(DE3)-RIPL, (C) Arctic Express (DE3), and (D) BL21 (DE3) pLysS. Only the pLysS cells showed visible expression of insoluble TbPLA₂ which was detected at 39 and 58 kDa on the SDS-PAGE gel.

In the *P. pastoris* expression system, both the full-length and truncated TbPLA₂ were successfully expressed in soluble forms, but the expression was weaker compared to *E. coli*. The constructs expressed in *P. pastoris* contained an N-terminal FLAG tag and a C-terminal e-GFP tag. The full-length TbPLA₂-eGFP migrated at 69 kDa on SDS-PAGE (Figure 5A), while the truncated protein with no signal peptide and TM portion migrated at 67 kDa (Figure 5B). The visible fluorescent bands in the washes of the full-length protein (black arrows on the UV gel of Figure 5A), and the 43 kDa bands seen on the Coomassie gels of Figure 5B (not visible on the corresponding UV gel), indicate that the eGFP tag was cleaved off during expression due to proteolytic cleavage since the purification buffers contained protease inhibitors. TbPLA₂-eGFP was prone to aggregation and Fos-Choline-12 was found to be the most effective detergent in preventing aggregation and adhesion of the protein to the membrane of the concentrator (Table S5, Figures S5 and S6).

3.4 | Purification of TbPLA₂ Expressed in Rosetta 2 Cells

Truncated TbPLA₂ without the signal peptide and TM portion was expressed with and without the mClover fusion tag in Rosetta 2 cells and purified to homogeneity (Table 1). The truncated TbPLA₂-mClover was soluble and appeared as 52 and 72 kDa proteins on SDS-PAGE. The 72 kDa protein may be aggregated or partially folded TbPLA₂, whereas the 52 kDa protein is likely the correctly folded TbPLA₂ (Figure 6A). Like the TbPLA₂-eGFP, TbPLA₂-mClover was prone to proteolytic cleavage in the *E. coli* cells as shown by the 27 kDa mClover bands on the SDS-PAGE gel (Figure 6A). It is unlikely that proteolysis occurred during purification since the buffer used contained protease inhibitors. Cleavage by TEV protease released free TbPLA₂ from both the 52 and 72 kDa proteins. The free TbPLA₂ migrated at 43 kDa on SDS-PAGE (Figure 6B). The free TbPLA₂ bands and the markers are

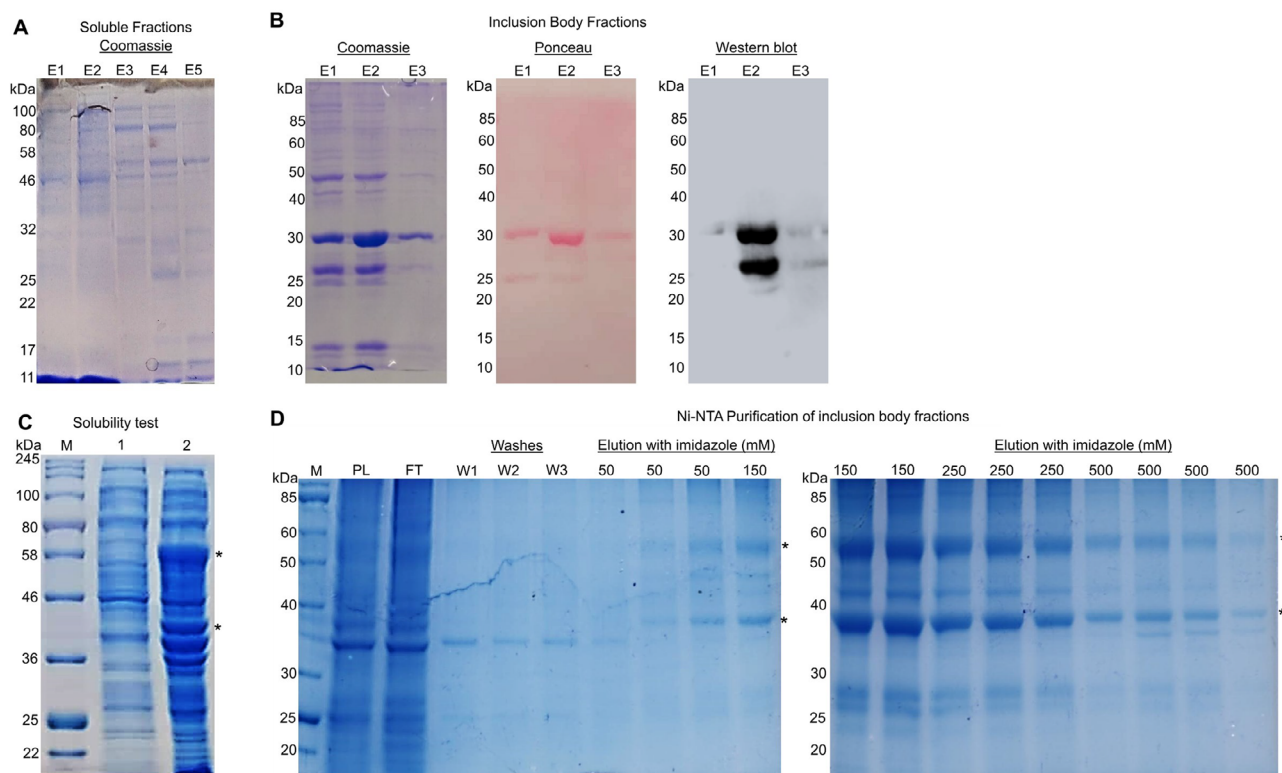


FIGURE 4 | Sodium dodecyl polyacrylamide gel electrophoresis (SDS-PAGE) of Ni-NTA-purified *Trypanosoma brucei* phospholipase A₂ (TbPLA₂) expressed in *E. coli* Cells: (A) TbPLA₂ was not detected in the soluble fractions of the lysed RIPL cells. E1–E5 = Ni-NTA column fractions. (B) Fractions purified from the solubilized RIPL inclusion body contained degraded TbPLA₂. The Coomassie and Ponceau stained gels, and Western blot with mouse anti-his monoclonal antibody confirmed the presence of degraded TbPLA₂. E1–E3 = Ni-NTA column fractions. (C) Solubility test using RIPA buffer for the lysis of the induced pLysS cells confirmed the deposition of TbPLA₂ in the inclusion bodies (pellet fraction). (D) Ni-NTA purification of TbPLA₂ from the solubilized pLysS inclusion body. The solubilized TbPLA₂ migrated at 39 and 58 kDa on SDS-PAGE. (E) Mobility Shift analysis of refolded TbPLA₂. R = reduced sample, NR = nonreduced sample (containing β-mercaptoethanol). The difference in the migration of the samples suggests restoration of disulfide linkages and renaturation of TbPLA₂.

TABLE 1 | Purification of TbPLA₂ expressed using pFLAG vector in Rosetta 2 cells.

Expression vector	Target protein	Step	Volume (mL)	Total protein (mg/mL)	Total activity (μmol/min)	Specific activity (μmol/min/mg)	Purification fold	Yield (%)
pFLAG	Truncated TbPLA ₂ -mClover	Lysate	547	424	18	0.042	1	100
		Supernatant	500	399	16	0.041	0.97	88.89
		Ni-NTA	36	16.2	15	0.926	22.04	83.33
		Post-TEV protease	15	0.282	12	54.54	1298	66.67
	Truncated TbPLA ₂	Lysate	1200	359.1	38	0.11	1	100
		Supernatant	1005	296	36	0.12	1.09	94.74
		Ni-NTA	25	0.56	35	107.14 ^a	974	92.11

Abbreviations: TbPLA₂, *Trypanosoma brucei* phospholipase A₂; TEV, tobacco etch virus.

^aThe specific activity of TbPLA₂ expressed without the mClover tag was two-fold higher than that of the TbPLA₂ released from mClover by TEV protease cleavage.

visible on the Coomassie-stained gel but not on the corresponding UV gel, as they are not fluorescent. TEV protease and mClover have similar molecular weights, approximately 27 kDa as seen on the gel. Aggregation of TbPLA₂ was also observed as shown by the smearing of the bands on the gel. This affected the TEV enzyme efficiency and the subsequent isolation of free TbPLA₂. The TEV-

cleaved TbPLA₂ has a specific activity of 54.54 μmol/min/mg (Table 1). Truncated TbPLA₂ without the mClover tag was finally expressed in Rosetta 2 cells. The protein migrated at 39 kDa on SDS-PAGE (Figure 6C) and exhibited high activity, with a specific activity of 107.14 μmol/min/mg, approximately twice that of the TEV-cleaved TbPLA₂.

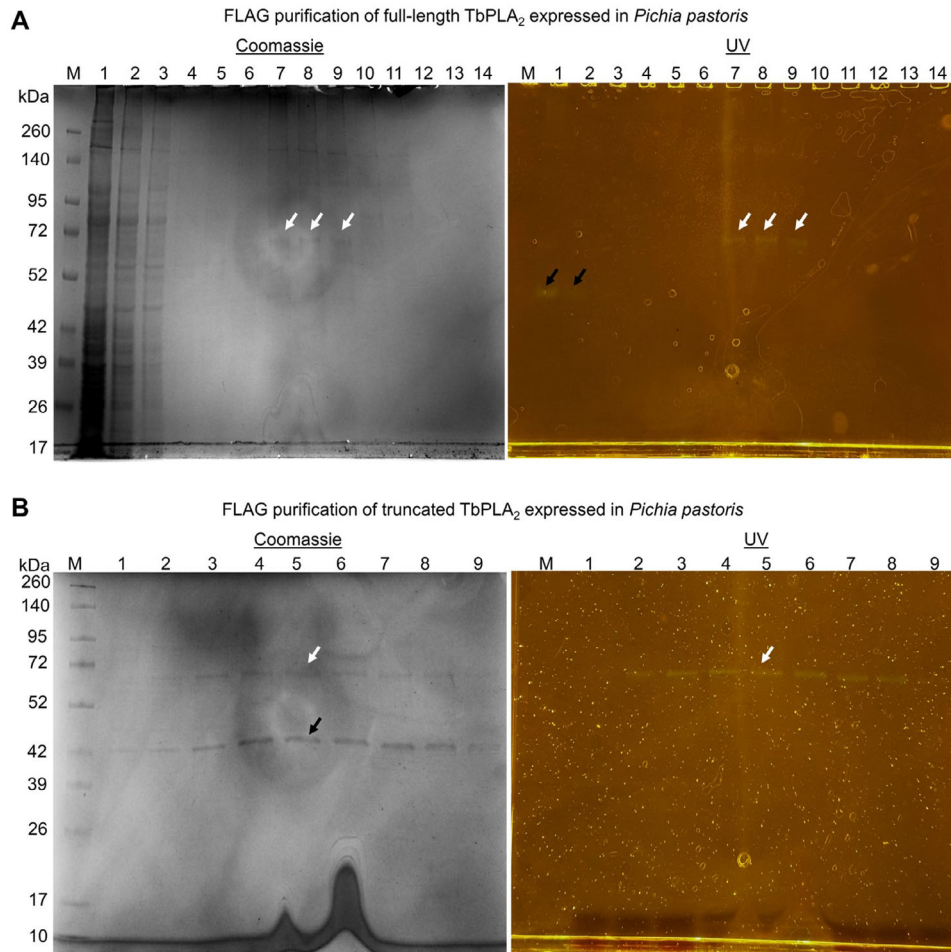


FIGURE 5 | Purification of *Trypanosoma brucei* phospholipase A₂ (TbPLA₂) expressed in *Pichia pastoris*: (A) 10% (w/v) sodium dodecyl polyacrylamide gel electrophoresis (SDS-PAGE) of purified full-length TbPLA₂ expressed in *P. pastoris*. Lanes: M = marker; 1–3 = washes; 4–15 = eluted fractions. The full-length TbPLA₂ (white arrow) migrated at 69 kDa. (B) 12% (w/v) SDS-PAGE of purified truncated TbPLA₂ expressed in *P. pastoris*. Lanes: M = marker; 1–9 = eluted fractions. The truncated recombinant TbPLA₂ migrated at 67 kDa (white arrows). Purification was done on FLAG M2 resin.

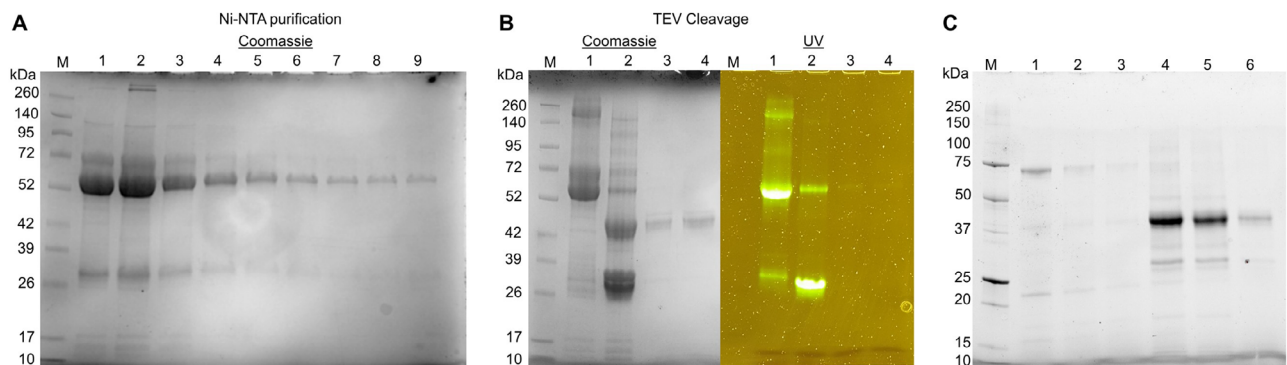


FIGURE 6 | Sodium dodecyl polyacrylamide gel electrophoresis (SDS-PAGE) of *Trypanosoma brucei* phospholipase A₂ (TbPLA₂)-mClover expressed in Rosetta 2 cells and purified on Ni-NTA. (A) Coomassie-stained gel of purified TbPLA₂-mClover. Lanes: M = marker; 1–9 = eluted fractions. (B) Coomassie-stained and UV gels of tobacco etch virus protease (TEV) cleavage reaction of TbPLA₂-mClover. Lanes: M = marker; 1 = uncut TbPLA₂-mClover; 2 = TEV-cleaved TbPLA₂-mClover; 3 and 4 = free TbPLA₂ isolated from post-TEV Ni-NTA cleanup step. The free TbPLA₂ and the marker are not visible on the UV gel because they are not fluorescent. TEV protease and mClover are approximately 27 kDa. (C) Coomassie-stained gel of purified truncated TbPLA₂ expressed in Rosetta 2 cells. Lanes: M = marker; 1–2 = washes; 3–7 = eluted fractions. The recombinant TbPLA₂ without its signal peptide and transmembrane domains migrated at 39 kDa on the SDS-PAGE gel.

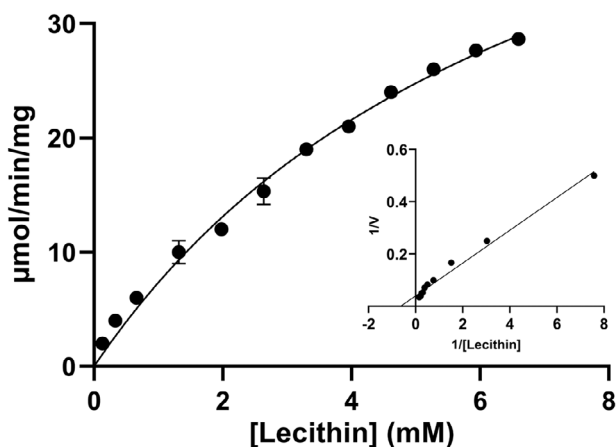


FIGURE 7 | Kinetic studies for the determination of K_M and V_{max} of *Trypanosoma brucei* phospholipase A₂ (TbPLA₂). The reciprocal of L- α -lecithin concentration ($1/[S]$) against the reciprocal of reaction velocity ($1/V$) was plotted to determine the kinetic parameters using a linear regression line. TbPLA₂ has a K_M of 1.58 mM and a V_{max} of 25.1 μ mol/min.

3.5 | Determination of Kinetic Parameters of TbPLA₂

The activity measurement data of recombinant TbPLA₂ at varying substrate concentrations were fitted for the Michaelis-Menten plot (Figure 7), which was transformed into a double-reciprocal plot (Figure 7 inset). The double reciprocal plot of velocity against substrate concentration for the hydrolysis of L- α -lecithin by TbPLA₂ showed that the K_M and V_{max} of TbPLA₂ were 25.1 μ mol/min and 1.58 mM, respectively.

4 | Discussion

PLA₂ is highly similar among the kinetoplastids but substantially different from the mammalian homologs positioning it as an excellent therapeutic target. Despite being a validated drug target, the difficulty in expressing soluble recombinant TbPLA₂ has limited its exploitation for therapeutic discovery [17, 29, 30]. Previous attempts to express full-length TbPLA₂ in *E. coli* and *Sf9* cells were unsuccessful [29]. We used genetic engineering and biophysical approaches to express TbPLA₂ in milligram quantity in *E. coli* and *P. pastoris* and characterize the soluble protein.

We optimized the *tbpla2* gene for the expression of its recombinant protein in *E. coli* [31, 32]. For high gene expression levels, a CAI of 1.0 is perfect in a desired expression system while a CAI greater than 0.8 is regarded as good. The optimized *tbpla2* has a CAI of 0.96 and an adjusted GC content of 57%. GC content is a predictor of mRNA stability [33, 34]. The TMHMM and I-TASSER predictions revealed the presence of a 30-amino acids signal peptide and two TM helices in TbPLA₂. These predictions guided the generation of the *tbpla2* constructs we used for the protein expression studies.

Except for the pLysS, the *E. coli* expression systems used in this study could not express full-length TbPLA₂ as the protein was heavily degraded and deposited as inclusion bodies. We

attributed this to the toxicity of TbPLA₂ and leaky expression of the BL21 expression systems. Heterologous expression of toxic membrane proteins that contain hydrophobic domains is usually challenging [29, 35]. The free fatty acids (FFAs) released from the hydrolysis of membrane phospholipids by PLA₂ exhibit detergent-like properties and can accumulate to toxic levels in *E. coli*, destabilizing its membrane and causing cell lysis [15]. The cytotoxic and hemolytic effect of FFAs released by PLA₂ on cells have been demonstrated [36]. Destruction of red blood cells by FFAs released by PLA₂ may contribute to the mechanisms of anemia in trypanosomiasis. The toxicity of TbPLA₂ may explain why it could not be expressed in soluble form in the *E. coli* cells [29].

To overcome these challenges, we expressed the full-length TbPLA₂ in BL21(DE3) pLysS cells which produces T7 lysozyme that inhibits T7 RNA polymerase, enabling tight control of gene expression. The pLysS expression system is ideal for expressing toxic proteins [37]. Background expression and degradation of TbPLA₂ were reduced in pLysS, but the protein was yet insoluble and remained in the inclusion bodies. The purified inclusion body protein was refolded and detected by immunoblotting using mouse anti-His monoclonal antibody as 39 and 58 kDa proteins. The mobility shift observed in the migration of the reduced and nonreduced samples of the refolded TbPLA₂ on SDS-PAGE suggests restoration of the disulfide linkages after refolding. We did not proceed with enzyme activity assay using the refolded protein but explored other options for the expression of soluble TbPLA₂.

Fusion tags are often used to enhance the solubility and stability of recombinant proteins. We expressed the full-length and truncated TbPLA₂ in fusion with N-terminal FLAG and C-terminal eGFP tags in *P. pastoris*. Soluble and active recombinant TbPLA₂ proteins were produced in *P. pastoris*, but the yield was poor, hence, the faint bands on the SDS-PAGE gel. The TbPLA₂-eGFP was prone to proteolytic cleavage and aggregation, making it difficult to isolate free TbPLA₂ from the eGFP after TEV cleavage. Most of the protein aggregated and was lost during concentration using centrifugal filters. The addition of 0.1% Fos-Choline-12 in the purification buffer reduced aggregation but did not completely prevent it. The presence of hydrophobic amino acids in the TbPLA₂ sequence, as predicted by the TMHMM analysis, may contribute to hydrophobic interactions that cause aggregation, thereby complicating the purification and isolation of free TbPLA₂ [19, 20].

Having encountered these problems, we made a truncated TbPLA₂ construct which lacks the signal peptide and TM sequences and subcloned it into the pFLAG vector. A C-terminal mClover and an N-terminal FLAG sequence present in the pFLAG backbone are expressed in fusion with the TbPLA₂. The protein yield in *E. coli* was better than in *P. pastoris*. Since the FLAG tag occupies the position of the removed TM sequences, it can serve as a scaffold mimicking the TM of TbPLA₂. FLAG tag is also an affinity tag for purification on anti-FLAG M2 affinity resin or western blot detection using anti-FLAG antibody. Like the TbPLA₂-eGFP, the TbPLA₂-mClover was also prone to proteolytic cleavage in Rosetta 2 cells. The mClover tag, unlike eGFP, is less sensitive to pH changes and less toxic to cells. The higher fluorescence intensity and photostability of mClover

make it easier to detect and monitor over longer periods. It also has a higher signal-to-noise ratio [38, 39]. As seen with eGFP, aggregation of mClover with TbPLA₂ also complicated TEV-cleavage and isolation of free TbPLA₂. The addition of 0.1% Fos-Choline-12 to the purification buffer reduced aggregation, particularly in small-scale purification. The TEV-cleaved TbPLA₂ has a specific activity of 54.54 $\mu\text{mole}/\text{min}/\text{mg}$. High concentration and increased intermolecular interactions are known to induce protein aggregation [40–42]. We performed TEV cleavage at lower TbPLA₂ concentrations, while factors that induce protein degradation such as extreme temperatures, pH, and prolonged exposure to light were avoided, but we were yet unable to successfully isolate free TbPLA₂. Isolation of TbPLA₂ by ion exchange chromatography, as well as desalting resulted in a complete loss of enzyme activity, likely due to the removal of Ca²⁺, which is essential for the enzyme's function. It is possible that interactions with the columns stripped the enzyme of bound calcium ions. Attempts to restore activity by adding CaCl₂ were unsuccessful.

Consequently, we removed the mClover tag and created a final TbPLA₂ construct that lacked the signal peptide and TM helices. This was expressed in Rosetta 2 cells and purified on Ni-NTA column. The purified TbPLA₂ migrated at 39 kDa on SDS-PAGE and has a specific activity of 107.14 $\mu\text{mole}/\text{min}/\text{mg}$, which is approximately two-fold of the specific activity of the free TbPLA₂ released from the mClover tag by TEV cleavage. Kinetic analysis of the recombinant TbPLA₂ revealed a V_{max} of 25.1 $\mu\text{mol}/\text{min}$ and a K_{M} of 1.58 mM.

5 | Concluding Remarks

This study has successfully developed a robust and effective protocol for overproducing active soluble TbPLA₂ using recombinant DNA technology approaches. The purification and kinetic analysis of TbPLA₂ will facilitate the discovery of its inhibitors and form a basis for developing novel therapeutics against African and American trypanosomiasis.

Acknowledgments

This research received substantial support from Emmanuel Balogun, Emmanuel Amlabu, and Geoffrey Chang. Emmanuel Oluwadare Balogun is a recipient of Emerging Global Leader (K43) Award and supported by the Fogarty International Center of the National Institutes of Health under award number K43TW012015. The content of this manuscript is solely the responsibility of the authors and does not necessarily represent the official views of the National Institutes of Health.

Conflicts of Interest

The authors declare no conflicts of interest.

Data Availability Statement

The data that support the findings of this study are available from the corresponding author upon reasonable request.

References

1. WHO, Trypanosomiasis, Human African (Sleeping Sickness). Fact Sheets [Online], (2023), accessed January 26, 2025, <https://www.who.int/news-room/fact-sheets/detail/trypanosomiasis-human-african-sleeping-sickness>.
2. M. Yaro, K. A. Munyard, M. J. Stear, and D. M. Groth, "Combating African Animal Trypanosomiasis (AAT) in Livestock: The Potential Role of Trypanotolerance," *Veterinary Parasitology* 225 (2016): 43–52.
3. E. O. Balogun, D. K. Inaoka, T. Shiba, et al., "Discovery of Trypanocidal Coumarins With Dual Inhibition of Both the Glycerol Kinase and Alternative Oxidase of *Trypanosoma brucei brucei*," *FASEB Journal* 33 (2019): 13002–13013.
4. R. Papagni, R. Novara, M. L. Minardi, et al., "Human African Trypanosomiasis (Sleeping Sickness): Current Knowledge and Future Challenges," *Frontiers in Tropical Diseases* 4 (2023): 1087003.
5. O. A. Adepoju, O. A. Afinowi, A. M. Tauheed, et al., "Multisectoral Perspectives on Global Warming and Vector-Borne Diseases: A Focus on Southern Europe," *Current Tropical Medicine Reports* 10 (2023): 47–70.
6. E. O. Balogun, A. J. Nok, and K. Kita, "Global Warming and the Possible Globalization of Vector-Borne Diseases: A Call for Increased Awareness and Action," *Tropical Medicine and Health* 44 (2016): 38.
7. M. Florin-Christensen, J. Florin-Christensen, E. D. de Isola, et al., "Temperature Acclimation of *Trypanosoma cruzi* Epimastigote and Metacyclic Trypomastigote Lipids," *Molecular and Biochemical Parasitology* 88 (1997): 25–33.
8. M. Wainszelbaum, E. Isola, S. Wilkowsky, et al., "Lysosomal Phospholipase A1 in *Trypanosoma cruzi*: An Enzyme With a Possible Role in the Pathogenesis of Chagas' disease," *Biochemical Journal* 355 (2001): 765–770.
9. M. L. Salto, L. E. Bertello, M. Vieira, et al., "Formation and Remodeling of Inositolphosphoceramides During Differentiation of *Trypanosoma cruzi* From Trypomastigote to Amastigote," *Eukaryot Cell* 2 (2003): 756–768.
10. A. C. Chagas-Lima, M. G. Pereira, P. Fampa, et al., "Bioactive Lipids Regulate *Trypanosoma cruzi* Development," *Parasitology Research* 118 (2019): 2609–2619.
11. I. Ishii, N. Fukushima, X. Ye, and J. Chun, "Lysophospholipid Receptors: Signaling and Biology," *Annual Review of Biochemistry* 73 (2004): 321–354.
12. J. J. van Hellemond and A. G. Tielens, "Adaptations in the Lipid Metabolism of the Protozoan Parasite *Trypanosoma brucei*," *FEBS Letters* 580 (2006): 5552–5558.
13. F. R. Oppendoerfer and J. van Roy, "The Phospholipases of *Trypanosoma brucei* Bloodstream Forms and Cultured Procyclics," *Molecular and Biochemical Parasitology* 5 (1982): 309–319.
14. A. Aloulou, Y. B. Ali, S. Bezzine, Y. Gargouri, and M. H. Gelb, "Phospholipases: An Overview," *Methods in Molecular Biology* 861 (2012): 63–85.
15. M. L. Belaunzaran, E. M. Lammel, and E. L. de Isola, "Phospholipases A in Trypanosomatids," *Enzyme Research* 2011 (2011): 1.
16. W.-Y. Ong, T. Farooqui, G. Kokotos, and A. A. Farooqui, "Synthetic and Natural Inhibitors of Phospholipases A₂: Their Importance for Understanding and Treatment of Neurological Disorders," *ACS Chemical Neuroscience* 6 (2015): 814–831.
17. M. N. Shuaibu, H. Kanbara, T. Yanagi, et al., "Phospholipase A₂ From *Trypanosoma brucei gambiense* and *Trypanosoma brucei brucei*: Inhibition by Organotin," *Journal of Enzyme Inhibition* 16 (2001): 433–441.
18. M. Bordon, M. D. Laurenti, S. P. Ribeiro, et al., "Effect of Phospholipase A(2) Inhibitors During Infection Caused by *Leishmania (Leishmania) amazonensis*," *The Journal of Venomous Animals and Toxins Including Tropical Diseases* 24 (2018): 21.

19. G. E. Tusnady and I. Simon, "Principles Governing Amino Acid Composition of Integral Membrane Proteins: Application to Topology Prediction," *Journal of Molecular Biology* 283 (1998): 489–506.
20. G. E. Tusnady and I. Simon, "The HMMTOP Transmembrane Topology Prediction Server," *Bioinformatics* 17 (2001): 849–850.
21. A. Krogh, B. Larsson, G. von Heijne, and E. L. Sonnhammer, "Predicting Transmembrane Protein Topology With a Hidden Markov Model: Application to Complete Genomes," *Journal of Molecular Biology* 305 (2001): 567–580.
22. X. Zhou, W. Zheng, Y. Li, et al., "I-TASSER-MTD: A Deep-Learning-Based Platform for Multi-Domain Protein Structure and Function Prediction," *Nature Protocols* 17 (2022): 2326–2353.
23. D. G. Gibson, H. O. Smith, C. A. Hutchison III, J. C. Venter, and C. Merryman, "Chemical Synthesis of the Mouse Mitochondrial Genome," *Nature Methods* 7 (2010): 901–903.
24. A. Y. Chang, V. Chau, J. A. Landas, and Y. Pang, "Preparation of Calcium Competent *Escherichia coli* and Heat-Shock Transformation," *JEMI Methods* 1 (2017): 22–25.
25. S. Wu and G. J. Letchworth, "High Efficiency Transformation by Electroporation of *Pichia pastoris* Pretreated With Lithium Acetate and Dithiothreitol," *Biotechniques* 36 (2004): 152–154.
26. E. O. Balogun, D. K. Inaoka, T. Shiba, et al., "Biochemical Characterization of Highly Active *Trypanosoma brucei gambiense* Glycerol Kinase, a Promising Drug Target," *Journal of Biochemistry* 154 (2013): 77–84.
27. M. Peach, N. Marsh, E. I. Miskiewicz, and D. J. MacPhee, "Solubilization of Proteins: The Importance of Lysis Buffer choice," in *Western Blotting: Methods and Protocols*, eds. B. T. Kurien and R. H. Scofield (Springer, 2015), 49–60.
28. M. K. Bhat and T. V. Gowda, "Purification and Characterization of a Myotoxic Phospholipase A₂ From Indian Cobra (*Naja naja naja*) Venom," *Toxicon* 27 (1989): 861–873.
29. K. Muhammad, "Identification and Characterization of Phospholipase A₂ From *Trypanosoma Brucei*," (Universität Tübingen, 2009), Accessed Januaray 26, 2025, <https://publikationen.uni-tuebingen.de/xmlui/handle/10900/43916?show=full>.
30. H. Memariani and M. Memariani, "Melittin as a Promising Anti-Protozoan Peptide: Current Knowledge and Future Prospects," *AMB Express* 11 (2021): 69.
31. S. T. Parvathy, V. Udayasuriyan, and V. Bhadana, "Codon Usage Bias," *Molecular Biology Reports* 49 (2022): 539–565.
32. G. Hanson and J. Collier, "Codon Optimality, Bias and Usage in Translation and mRNA Decay," *Nature Reviews Molecular Cell Biology* 19 (2018): 20–30.
33. F. Hia, S. F. Yang, Y. Shichino, et al., "Codon Bias Confers Stability to Human mRNAs," *EMBO Reports* 20 (2019): e48220.
34. V. Presnyak, N. Alhusaini, Y. H. Chen, et al., "Codon Optimality Is a Major Determinant of mRNA Stability," *Cell* 160 (2015): 1111–1124.
35. R. Laage and D. Langosch, "Strategies for Prokaryotic Expression of Eukaryotic Membrane Proteins," *Traffic (Copenhagen, Denmark)* 2 (2001): 99–104.
36. C. M. Colley, R. F. Zwaal, B. Roelofsen, and L. L. van Deenen, "Lytic and Non-Lytic Degradation of Phospholipids in Mammalian Erythrocytes by Pure Phospholipases," *Biochimica et Biophysica Acta (BBA)—Biomembranes* 307 (1973): 74–82.
37. S. H. Pan and B. A. Malcolm, "Reduced Background Expression and Improved Plasmid Stability With pET Vectors in BL21 (DE3)," *Biotechniques* 29 (2000): 1234–1238.
38. A. J. Lam, F. St-Pierre, Y. Gong, et al., "Improving FRET Dynamic Range With Bright Green and Red Fluorescent Proteins," *Nature Methods* 9 (2012): 1005–1012.
39. B. C. Campbell, G. A. Petsko, and C. F. Liu, "Crystal Structure of Green Fluorescent Protein Clover and Design of Clover-Based Redox Sensors," *Structure* 26 (2018): 225–237.
40. H. C. Mahler, W. Friess, U. Grauschopf, and S. Kiese, "Protein Aggregation: Pathways, Induction Factors and Analysis," *Journal of Pharmaceutical Sciences* 98 (2009): 2909–2934.
41. M. Hofmann, M. Winzer, C. Weber, and H. Gieseler, "Prediction of Protein Aggregation in High Concentration Protein Solutions Utilizing Protein-Protein Interactions Determined by Low Volume Static Light Scattering," *Journal of Pharmaceutical Sciences* 105 (2016): 1819–1828.
42. Y. Baek and A. L. Zydney, "Intermolecular Interactions in Highly Concentrated Formulations of Recombinant Therapeutic Proteins," *Current Opinion in Biotechnology* 53 (2018): 59–64.

Supporting Information

Additional supporting information can be found online in the Supporting Information section.